Available online at www.sciencedirect.com

ScienceDirect

Procedia CIRP 95 (2020) 891–896

www.elsevier.com/locate/procedia

20th CIRP CONFERENCE ON ELECTRO PHYSICAL AND CHEMICAL MACHINING

Laser Surface Texturing of PECM Tools and the Validation

Shiqi Fang[a,b,] *, Alexander Ernst[a], Luis Llanes[b], Dirk Bähre[a]

[a]*Institute of Production Engineering, Saarland University, Saarbrücken 66123, Germany*
[b]*CIEFMA – Dept. Materials Science and Engineering, EEBE-Universitat Politècnica de Catalunya, Barcelona 08019, Spain*

* Corresponding author. Tel.: +49(0)6813023727; fax: +49(0)6813024858. *E-mail address:* shiqi.fang@uni-saarland.de

Abstract

As a non-contact unconventional machining approach, Electrochemical Machining (ECM), it is widely used for the machining of modern high-strength materials in the automotive, aerospace, or medical industry. ECM is also considered as an effective approach to reproduce complex surface patterns on the workpieces with high geometrical precision. On the other hand, it becomes a practical demand to precisely produce the desired pattern molds on the ECM tools, i.e., cathodes. Compared to traditional cathode forming approaches, such as milling, a short-pulsed laser can shape or sculpture functional surfaces on the scale of micrometers. In this study, a nanosecond laser was implemented to produce several complex two- and three-dimensional patterns on the PECM cathodes, made of the stainless steel 1.4301, including grooves, half spheres, and hexagonal pyramids. The textured tools were tested and validated on an industrial PECM machine *PEMCenter8000*, by replicating those patterns on workpieces made of Ti-6Al-4V. In this paper, fabrication of the tool patterns using nanosecond laser and ~~and the~~ subsequent quality inspection are introduced, and the first results of the tool validation are presented by comparing the geometrical measurement of the tool patterns to those replicated on the workpieces. It is found that the tool patterns produced by the nanosecond laser have clear surface conditions, and the tool pattern shapes meet the initial design. The geometrical precision of the pattern replications on the workpieces could be strongly influenced by the pattern design, as those sharp edges could cause an anisotropic electric field and instable electrolyte flushing conditions. The molten materials staked on the sharp positions might also be an important factor.

Keywords: PECM; nanosecond laser; surface texturing; geometrical precision, surface integrity.

1. Introduction

The constantly growing demand for high-performance products, e.g., in the automotive or aerospace sectors, leads to further development on the product quality and performances. Challenges arise during the manufacture of these products in order to meet the increasing demands not only on the material properties, e.g., special mechanical or thermal properties but also on the functional properties of the product surfaces, e.g., tribological properties. Within this regard, sophisticated patterns should be fabricated on those high-strength materials without hurt their integrity.

Due to the mechanical contactless nature, Pulse Electrochemical Machining (PECM) is predestined to machine these materials on a micron-scale without inducing any mechanical or thermal loads. During this process, the geometrical features of products are directly determined by the producible quality of the tool. Within this regard, the tool is of great importance to achieve the aimed properties of the product. Therefore, some alternative process chains are needed for tool manufacturing.

Laser surface texturing (LST) is a clean and fast surface treatment approach, especially suitable for functional surfaces with high demand on the geometrical complexity and precision on the scale of micrometers [1,2]. The applications of LST is now emerging in traditional metal shaping or functionalization processes. It is reported that special motifs, such as grooves and dimples, produced on the cutting parts of cutting tools,

10.1016/j.procir.2020.01.183

improved the tribological performances effectively, like the lubricant distribution [3-5]. There are also examples of surface texturing on the grinding disks to improve the tool conditionings [6,7]. It has been successfully attempted to implement hardmetals in the abrasive machining processes through the replication of similar topographic features of a honing stone on the working surfaces using short-pulsed lasers [8,9].

Regarding the non-conventional machining processes, there is new research on the fabrication of functional surface structures, such as dimples or grooves, using ECM or combining with laser beams [10,11]. However, most of those surface structures produced by ECM in recent studies are based on the two-dimensional processing and, the resulting geometrical features, including dimension and precision, is also quite limited. A significant factor of the limitation is linked to the fabrication of the tool shape as the mold of the surface structures. In previous studies, the use of non-conventional manufacturing processes, such as electrochemical discharge machining [12] or photolithography [13,14], were attempted to fabricate micro-textured tools of PECM and achieved good results. In this study the nanosecond laser integrated in the micromachining platform has been applied to fabricate specific two- and three-dimensional textures on the ECM tools. Validation of those textured tools has been carried out through the replication tests on an industrial PECM machine. The first results show a satisfactory agreement of the geometrical features between the tools and the workpieces in the case of the reproduction of spherical structures. The reproduction of sharp-edged patterns using PECM is still challenging as obvious deviations of some geometrical features occurred between tools and workpieces.

2. Materials and Equipment

2.1. Materials studied and sample preparation

The PECM tool samples, made of the stainless steel 1.4301 (Table 1), have a rotary connection to the spindle, as shown in Figure 1. The detachable design facilitates the necessary montage during the laser processing and geometrical measurements. The working surfaces have a diameter of 12 mm, and they were finely polished prior to the laser texturing. As anode (workpiece electrode), Ti-6Al-4V was chosen. The chemical compositions of the tool and workpiece material are listed in Table 1.

Table 1. Chemical composition of the applied tool, stainless steel 1.4301, and workpiece material, Ti-6Al-4V (in wt%).

1.4301 (in wt%)						
C	Si	Mn	S	Cr	Ni	Fe
≤0.07	1.0	2.0	0.03	18.0	10.0	bal.

Ti-6Al-4V (in wt%)						
C	N	O	H	V	Al	Ti
≤0.08	≤0.05	≤0.2	≤0.015	6.00	4.00	bal.

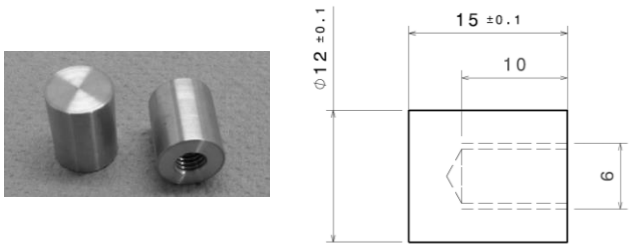

(a) (b)

Figure 1. (a) PECM tool samples with detachable design, (b) detailed dimensions of the samples.

2.2. Experimental equipment

2.2.1. Nanosecond laser setup

The micromachining platform, as shown in Figure 2(a), consists of the nanosecond laser setup (solid-state Nd:YLF, Q-switched, Explorer® One™ Spectra-Physics) combined with a two-axis laser beam deflection unit (Raylase), which enables the three-dimensional movement of laser beams in certain extend. The nanosecond laser setup can emit the laser beams with a wavelength of 349 nm and a pulse duration of five nanoseconds (FWHM, namely Full Width at Half Maximum), and the laser repetition frequency is one KHz, summarized in Table 2. The composition of the laser micromachining platform is illustrated in Figure 2, whereby the emitted laser beam is reflected by a series of mirrors and focused on the samples, pasted on the sample holder.

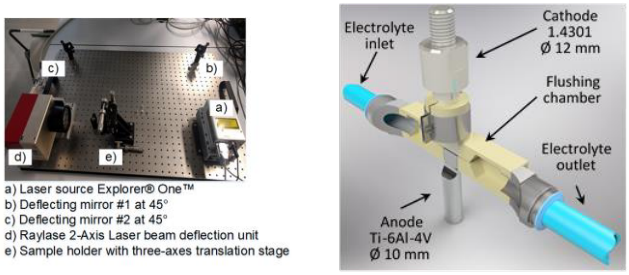

(a) (b)

Figure 2. (a) Configuration of the precise laser machining platform, (b) experimental unit integrated into PECM installation for the replication of surface patterns.

Table 2 Laser parameters used in this study.

Laser type	Laser source	Pulse duration (ns)	Wave length (nm)	Frequency (Hz)
ns-laser	Nd:YLF	5	349	1000

2.2.2. PECM setup

The pattern replication was carried out on an industrial pulse electrochemical machining installation PEMCenter8000 (PEMTec SNC, Forbach, France). As shown in Figure 2(b), an experimental unit integrated into a PECM machine consists of a 3D-printed flushing chamber and two electrodes, which are concentrically positioned. The electrolyte is supplied with a certain velocity and pressure flushing through the chamber in a single direction. This unit can obtain equal flushing conditions during the whole experiment.

3. Experimental aspects

3.1. Laser surface texturing

The precision and efficiency of the laser surface texturing are usually the results of many different combined factors, including intrinsic laser configuration, e.g., wavelength and pulse duration, and machining parameters, e.g., overlap and scan speed. The intrinsic laser configuration determines the laser-matter reaction mechanism. For example, the absorption of laser energy is, in general, inversely proportional to the wavelength for metals [15]. In practice, those intrinsic parameters of laser are often configured before the processing. On the other hand, the machining parameters determine the geometric outcome directly. Within this regard, the parameter spot overlap, related to the laser scanning strategies, is discussed to understand the achievement of those patterns.

Spot overlap is a dimensionless index, describing the superposition of two adjacent imprints subsequently generated by laser spot in the processing movement, as illustrated in Figure 3(a). The index interprets intuitively the quality of the scan track induced by the laser beams, and a smoother machining track can be achieved by a high overlap [8,16]. In practice, the index can be calculated using the equation:

$$U = 1 - \frac{v}{f_z \cdot D} \quad (1)$$

U: overlap in percentage
v: scan speed (mm/s)
D: spot size (µm)
f_z: pulse repetition frequency (Hz)

Other relevant laser machining parameters, including pulse energy, scan mode, scan speed, and filling speed, are given in Table 3. Knowing the spot size is 35 µm, the overlap is obtained to be 76%, i.e., corresponding approximately to 27 µm.

Table 3. Machining parameters of the nanosecond laser setup.

Pulse energy (µJ)	Scan mode	Scan speed (µm/ms)	Fill spacing (µm)	Spot overlap
100	Line by line	8.4	6	57 %

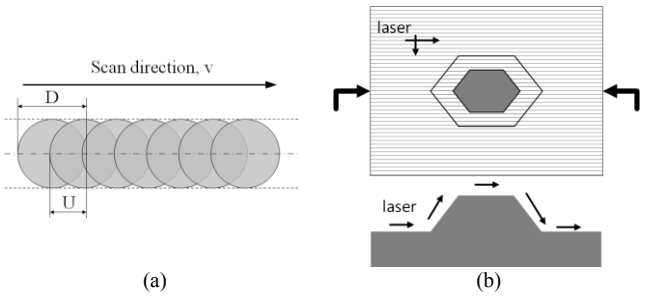

Figure 3. (a) Decomposition of the laser beam in the processing movement, (b) configuration of laser beam paths for the production of the three-dimensional patterns, here hexagonal pyramid as an example.

Three surface patterns (Figure 4), including the two-dimensional groove pattern, three-dimensional half-spheres, and hexagonal pyramids, were produced using the nanosecond laser setup. The groove is generated by the simple linear scanning of a laser beam. It is one of the most basic patterns in laser surface texturing, as complex geometry can be produced by different compositions of such linear scanning movement. On the other hand, the spot overlap can be evaluated directly by the groove pattern. The other two patterns with complex geometry, i.e., half-sphere and pyramid, are also involved. They deem to explore the influence of the geometrical features, i.e., straightness and curvature, on the pattern reproduction in the PECM processing.

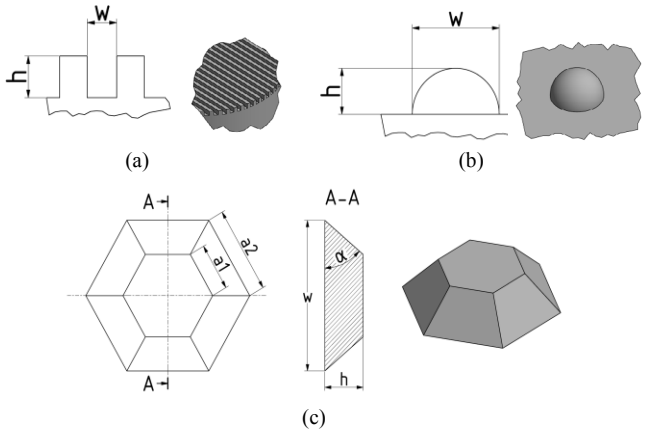

Figure 4. Design and dimension of the three patterns to be produced by laser: (a) grooves, (b) half-spheres, and (c) hexagonal pyramids. Whereby:

$a_{1,2}$: side length of the hexagonal pyramids
w: width of the grooves/half spheres
h: height/depth of the patterns
α: slope angle at the symmetric position of the hexagonal pyramids

According to the geometrical features of the patterns, specific routes of the laser beam movement are configured based on the line by line scan mode. In general, the laser beam moves on the XY-plan at the configured velocity in one direction, for example, from left to right, as shown in Figure 3(b). When the scanning is finished, the laser spot jumps to the next line, usually perpendicular to the scanning direction. For the two-dimensional grooves, the laser emission is continuous during the scanning. However, the emission is switched off synchronously for the production of the three-dimensional spheres or pyramids, when the laser beam passes through the convex parts of the patterns. Repetitions are then carried out in the direction of the Z-axis to sculpture the 3D half spheres or pyramids.

3.2. Pattern reproduction by PECM

Table 4. Process parameters used for the PECM replication experiments.

Geometric characteristic	Level
Process voltage U [V]	18.70
Feed rate vf [mm/min]	0.11
Pulse on-time ton [ms]	1.00
Mech. frequency fmech. [Hz]	50.00
Electr. frequency felectr. [Hz]	50.00
Electrolyte pressure p [kPa]	100.00
Electrolyte temperature T [°C]	22.00 ± 1.50
Electrolyte conductivity σ [mS/cm]	110.00 ± 5.00
pH value [-]	8.50 ± 0.20

Under the consideration that the pattern dimension is on the

scale of micrometers, it is advisable to configure a small gap between tool and workpiece, i.e., 20 µm for this experiment, in order to achieve satisfactory dimensional and shape precision in the pattern replication. Detailed process parameters determined in preliminary experiments are presented in Table 4, and a $NaNO_3$ based solution was chosen as the electrolyte in this study.

4. Results and discussion

4.1. Morphological inspection on the laser textured tools

Morphological features of the laser textured tools (T) have been inspected by the scanning electron microscope (SEM), as shown in Figure 5. In general, the workpiece surfaces after laser processing have a rather clear condition, exhibiting the border between the processed and unprocessed zones. The obtained shapes, i.e., grooves, half-spheres, and hexagonal pyramids, meet the initial shape designs and quality requirements at the first blink. The grooves were generated by a two-dimensional movement of the laser beams, i.e., continuously moving from the left to the right, as shown in Figure 5(b). The interval between the spot traces, i.e., spot overlap, is measured about 26.2 µm, close to the theoretical value of 27 µm, calculated in Section 3.1. Some side effects induced by the nanosecond laser are also observed, such as the molten materials covering the grooves and also staked at both groove borders (Figure 6(a)). The formation of such stack is linked to the energy distribution and the movement of the laser beams. The applied laser beams have a Gaussian profile, where the energy maxima are found in the profile middle and degrade alongside the profile. Therefore, the energy applied near to the borders might not be sufficient to evaporate the material but only to melt it. As the laser beam is moving forwards, the molten materials are pushed aside, and the stack is formed along with the molten materials cooled down. Similar scenarios are also remarkable on the borders of the pyramids, and discontinuity can also be observed on the sphere tops (Figure 5(c-f)). The stack may be mixed with the oxide of the materials, having rather brittle structures. In addition, both sides of the groove do not become a right angle but are tapered as a result of the profile of the laser. These tapers negatively impact not only the geometrical precision of laser textured patterns, but also the replication precision of workpieces in the PECM processes (Figure 6(b)).

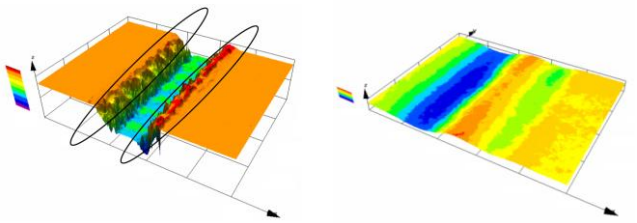

(a) (b)

Figure 6. Cross-sectional analysis of (a) laser-textured groove tool and (b) the corresponding electrochemically machined workpiece (different colors present the depth scale), schematic illustration as referred in Figure 8.

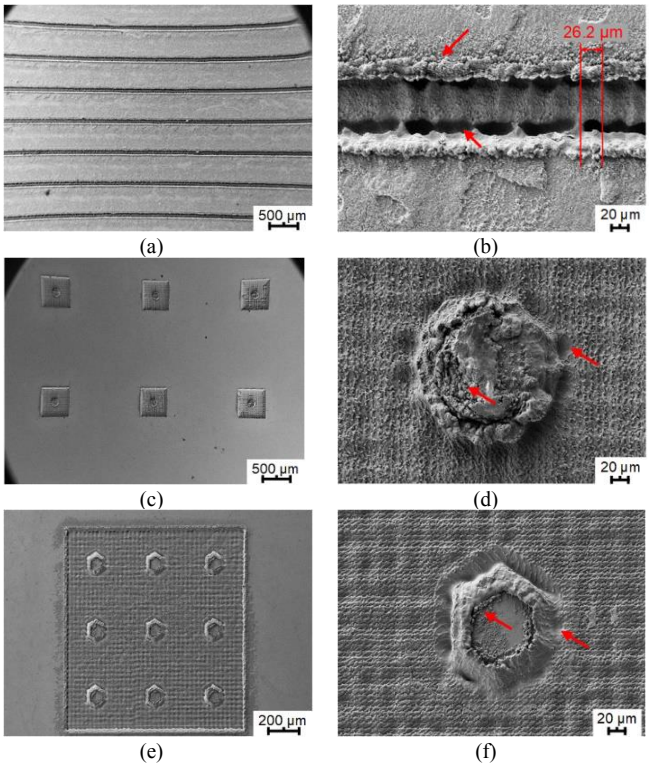

(a) (b) (c) (d) (e) (f)

Figure 5. Overview and local zoom of morphological inspections on the tools (T): (a) and (b) grooves, (c) and (d) half-spheres, (e) and (f) hexagonal pyramids.

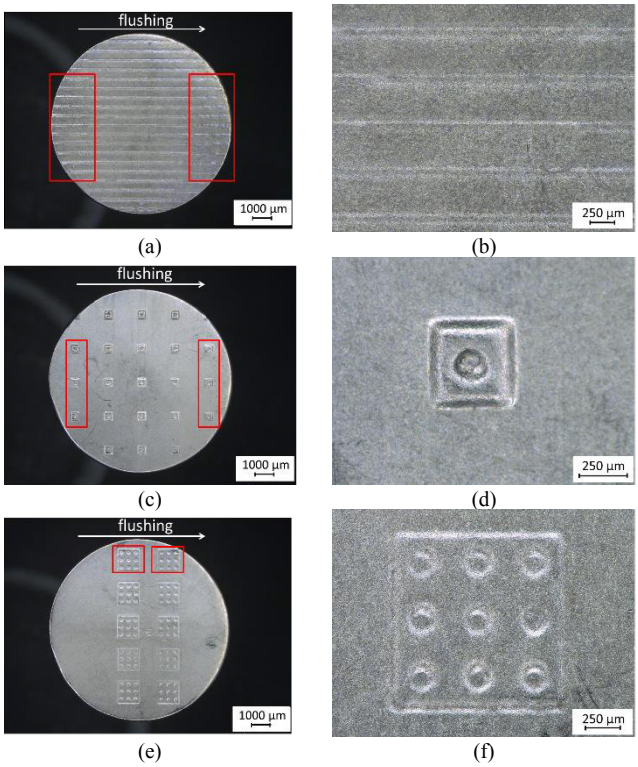

(a) (b) (c) (d) (e) (f)

Figure7. Overview and local zoom of morphological inspections on the electrochemical machined workpieces (W): (a) and (b) grooves, (c) and (d) half spheres, (e) and (f) hexagonal pyramids.

4.2. Morphological inspection on the electrochemically machined workpieces

The workpieces machined by the PECM were inspected using a digital microscope *Keyence VHX-500F* (Keyence Corporation, Nagoya, Japan), as shown in Figure 7. It is obvious that the grooves and hexagonal pyramids, having straight and sharp edges, exhibit blurred borders compared to the half spheres. This can be explained by considering the schematic representation of the formation of electrical field lines when using the groove tool (Figure 8). It becomes clear that the stack of the molten materials on the groove borders leads to a local concentration of the electrical field lines provoking an increase of the material removal on the workpiece. This unequal material removal compared to the surrounding area leads to the shape deviations observed, i.e., enlarged width and shallower height, in the replication experiments of the groove pattern (Figure 6(b)).

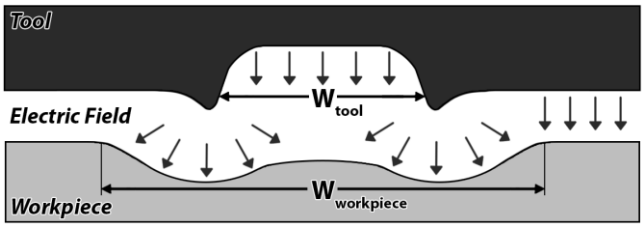

Figure 8. Schematic illustration of the electric removal mechanism between the tool and workpiece.

On the contrary, soft edges can achieve a better shape reproducibility, since such geometrical features allow to build up not only an isotropic electric field and but also a smooth electrolyte flushing behavior. In addition, the molten materials stacked at those sharp edges, i.e., on the borders of the grooves and pyramids, made the observations even more pronounced.

The macroscopic effect of the electrolyte flushing direction on the geometry reproduction can be detected on all the three patterns. The produced patterns close to the electrolyte inlet (left image area, marked in rectangle) exhibit better shape features than those close to the electrolyte outlet (right image area, marked in rectangle), where the performance of the electrolyte is degraded as the result of the contamination of the particles expelled from the workpieces. As the electrochemical reaction goes on, those removed particles and resulting process gases become more significant along the flushing direction, and such cumulative effects will increasingly weaken the electrical conductivity and therefore result in the local material removal instability.

4.3. Evaluation of the geometrical precision

In order to evaluate the geometrical precision of the pattern reproduction by PECM, the geometrical parameters listed in Figure 4 were measured on the tools (T) and the electrochemically machined workpieces (W) for each specific surface pattern, respectively, and their relative deviations (Δ) between tools and workpieces were accordingly calculated. The measurements were done with an Olympus LEXT OLS 3100 confocal laser scanning microscope (Olympus, Tokyo, Japan). Four measurements were conducted at different positions on each sample surface in order to get reliable values, and the obtained average values are listed in Table 5.

The geometrical measurement results, in general, confirm the morphological inspections in section 4.2. Large deviations, i.e., enlarged width and shallower height, were observed on the groove pattern with a value of 62.56 % in depth and 166.48 % in width. The sharp edge design and the stack of the molten materials on the groove borders increased local material dissolution and consequently formed rather blurred pattern borders on the workpieces. In contrast to the groove pattern, the half-sphere pattern achieved better precision with a relative deviation of 9.28 % in depth and 19.25 % in width. The relative deviation in width is approximately in the range of the gap distance 20 µm between tool and workpiece and can, therefore, be explained by the process characteristics of the PECM. Due to the contactless machining process, an exact mirror image transfer of the structures is not possible. The structure on the workpiece thus deviates from the structure of the tool by at least the amount of the gap distance. The small deviation in depth might be elaborated by the poorer electrolyte flushing conditions at the bottom of the spheres. This means that fewer electrolytes will be flushed through the bottom of the spheres than around the spheres. Thus, more material is removed from the sphere bottom than from around the sphere.

Table 5. Measurement results of tool (T) and workpiece (W) and the relative deviation (Δ) between tool and workpiece.

Pattern		Geometric characteristic				
		h [µm]	w [µm]	a_1 [µm]	a_2 [µm]	α [°]
Grooves	T	50.48	73.18	-	-	-
	W	18.90	195.00	-	-	-
	Δ [%]	62.56	166.48	-	-	-
Half spheres	T	34.39	132.08	-	-	-
	W	31.20	157.50	-	-	-
	Δ [%]	9.28	19.25	-	-	-
Hexagonal pyramids	T	7.10	-	82.86	38.72	8.09
	W	6.49	-	89.10	46.26	4.59
	Δ [%]	8.58	-	7.53	19.46	43.28

The geometrical features of the produced pyramids turned out to be critical: satisfactory precision has been achieved with deviations less than 10% in depth and side length a_1 at the bottom position on the tool, i.e., on the top position of the workpieces. However, the deviation of the obtained side length a_2 at the top position of the tool, which 'penetrated' into the workpiece, was still obvious. As shown in Figure 7 (e) and (f), due to the very poorly reproduced contours, the parameter a_2 could hardly be evaluated. On the one hand, the deviations of the side length might have resulted from the poor reproducibility of sharp edges by PECM. On the other hand, the molten materials stacked on the top sides of the pyramids, as shown in Figure 5(f), reinforced the disorder of the electric fields. As a result, the reduction of the angle α results from the reduced height and increased width of the structures.

5. Conclusion and discussion

In this study, it has been attempted to produce complex two- and three-dimensional patterns on ECM tools using a nanosecond laser setup. Meanwhile, the reproducibility of the patterned tools has been validated using an industrial PECM installation.

It is proven that the nanosecond laser is able to produce geometrically defined patterns on a micrometer scale on ECM tools with satisfactory geometrical precision in both two- and three-dimensions. The experimental results of the pattern reproductions on the PECM installation show an acceptable agreement of the geometrical features between the tools and the workpieces. However, deviations were still found on several geometrical parameters, linking to the sharp edges of the patterns, e.g., the groove borders and the pyramid sides.

In the electrochemical reaction, such edges can easily break the balance of the isotropic electric field alignment and change the smooth electrolyte flushing condition. As a result, different material removal rates are produced at those places. Meanwhile, molten materials induced by the laser were often stacked at those sharp edges, and they can worsen such unbalance. Therefore, it is recommendable in the future to improve the reproducibility in two aspects: reducing melting in the laser surface texturing and avoiding sharp edges in the pattern design. The use of pico- or femtosecond lasers with less thermal effects should also be considered.

Acknowledgements

The work leading to this publication was supported by the German Research Foundation (DFG) within the Individual Research Grant [425923019] “Laser Surface Textured Cemented Carbides for Application in Abrasive Machining Processes”.

References

[1] Etsion, I., 2005, State of the Art in Laser Surface Texturing, Journal of Tribology, 127/1:248, DOI:10.1115/1.1828070.

[2] Kapłonek, W., Nadolny, K., 2015, Laser methods based on an analysis of scattered light for automated, in-process inspection of machined surfaces: A review, Optik, 126/20:2764–2770, DOI:10.1016/j.ijleo.2015.07.009.

[3] Arslan, A., Masjuki, H. H., Kalam, M. A., Varman, M., Mufti, R. A., et al., 2016, Surface Texture Manufacturing Techniques and Tribological Effect of Surface Texturing on Cutting Tool Performance: A Review, Critical Reviews in Solid State and Materials Sciences, 41/6:447–481, DOI:10.1080/10408436.2016.1186597.

[3] Fang, S., Herrmann, T., Rosenkranz, A., Gachot, C., Marro, F. G., et al., 2016, Tribological Performance of Laser Patterned Cemented Tungsten Carbide Parts, Procedia CIRP, 42/Isem Xviii:439–443, DOI:10.1016/j.procir.2016.02.228.

[4] Ibatan, T., Uddin, M. S., Chowdhury, M. A. K., 2015, Recent development on surface texturing in enhancing tribological performance of bearing sliders, Surface and Coatings Technology, 272:102–120, DOI:10.1016/j.surfcoat.2015.04.017.

[5] Geiger, M., Popp, U., Engel, U., 2002, Excimer laser micro texturing of cold forging tool surfaces - Influence on tool life, CIRP Annals - Manufacturing Technology, 51/1:231–234, DOI:10.1016/S0007-8506(07)61506-6.

[6] Li, H. N., Axinte, D., 2016, Textured grinding wheels: A review, International Journal of Machine Tools and Manufacture, 109:8–35, DOI:10.1016/j.ijmachtools.2016.07.001.

[7] Walter, C., Komischke, T., Kuster, F., Wegener, K., 2014, Laser-structured grinding tools - Generation of prototype patterns and performance evaluation, Journal of Materials Processing Technology, 214/4:951–961, DOI:10.1016/j.jmatprotec.2013.11.015.

[8] Fang, S., Pérez, V., Salán, N., Baehre, D., Llanes, L., 2019, Surface Patterning of Cemented Carbides by Means of Nanosecond Laser, Materials and Manufacturing Processes, pp. 1–7, DOI:10.1080/10426914.2019.1628268.

[9] Fang, S., Llanes, L., Bähre, D., 2018, Laser surface texturing of a WC-CoNi cemented carbide grade: Surface topography design for honing application, Tribology International, 122:236–245, DOI:10.1016/j.triboint.2018.02.018.

[10] Chen, C., Li, J., Zhan, S., Yu, Z., Xu, W., 2016, Study of Micro Groove Machining by Micro ECM, Procedia CIRP, 42:418–422, DOI:10.1016/j.procir.2016.02.224.

[11] Sun, A., Chang, Y., Liu, H., 2019, Fabrication of hole without recast layer on coated alloy by using laser and electrochemistry, Optik, 179:285–297, DOI:10.1016/j.ijleo.2018.10.006.

[12] Steuer, P., Weber, O., Bähre, D., 2015, Structuring of wear-affected copper electrodes for electrical discharge machining using Pulse Electrochemical Machining, International Journal of Refractory Metals and Hard Materials, 52:85–89, DOI:10.1016/j.ijrmhm.2015.05.003.

[13] Weinmann, M., Weber, O., Bähre, D., Munief, W., Saumer, M., et al., 2014, Photolithography - electroforming - pulse electrochemical machining: An innovative process Chain for the high precision and reproducible manufacturing of complex microstructures, International Journal of Electrochemical Science. International Journal of Electrochemical Science, 9: 3917-3927.

[14] Natter, H., Weinmann, M., Munief, W., Weber, O., Bähre, D., Saumer, M., 2014, PhoGaTool: a new process chain for manufacturing of ecm tools, Proceedings of the 10th International Symposium on Electrochemical Machining Technology, 147-157, ISBN 978-3-95735-010-7.

[15] Dumitru, G., Lüscher, B., Krack, M., Bruneau, S., Hermann, J., et al., 2005, Laser processing of hardmetals: Physical basics and applications, International Journal of Refractory Metals and Hard Materials, 23/4-6 SPEC. ISS.:278–286, DOI:10.1016/j.ijrmhm.2005.04.020.

[16] Fang, S., Klein, S., 2019, Surface structuring of polycrystalline diamond (PCD) using ultrashort pulse laser and the study of force conditions, International Journal of Refractory Metals and Hard Materials, 84:105036, DOI:10.1016/j.ijrmhm.2019.105036.